BACHELOR

Mini Cyclone

Iron Powder Sampler After Combustion

Muijen, Lars L.

Award date:
2023

EINDHOVEN UNIVERSITY OF TECHNOLOGY

Department of Mechanical Engineering

Mini Cyclone

Iron Powder Sampler After Combustion

L.L. Muijen 1619322

Project supervisors: Mark Hulsbos
Helen Prime

Assessor Dr. Ing. R.T.E. Hermanns

Eindhoven, July 2, 2023

Contents

List of Symbols

Symbol	Variable	Unit
A	Area	m^2
a	Cyclone inlet height	m
$\tilde{b}$	Cyclone inlet width	m
β	Regression model parameters	-
C_D	Air resistance coefficient	-
D	Cyclone scale	m
D_c	Cyclone diameter	m
D_i	Cyclone inlet diameter	m
D_o	Cyclone outlet diameter	m
d_p	Particle diameter	m
$d_{p,50\%}$	Particle cut-off diameter	m
$\tilde{d}_r$	Cyclone outlet diameter ratio	-
ϵ	Error	Pa, m
F_{buo}	Buoyancy force	N
F_c	Centrifugal force	N
F_d	Resistance force	N
$\tilde{F}_s$	Contact surface area	m^2
f_0	Friction coefficient	-
H	Cylindrical height cyclone	m
K_A	Inlet area ratio	-
k_i	Correction coefficient of expansion loss	-
L	Cyclone total inner height	m
l	Vortex finder height	m
m_G	Mass gas	kg
m_p	Mass particle	kg
n_s	Swirl exponent	-
ΔP, Δp	Pressure loss	Pa
ρ_g	Gas density	kg/m^3
ρ_p	Particle density	kg/m^3
Q	Flow rate	m^3/s
Re	Reynolds number	-
r	Radius	m
μ	Viscosity	$N\,s/m^2$
V_c	Axial cyclone velocity	m/s
V_i	Inlet velocity	m/s
$V_{\theta w}$	Tangential velocity	m/s
$V_{r,e}$	Radial velocity outlet	m/s
V_{ze}	Axial velocity outlet	m/s
v_{TC}	Terminal velocity	m/s
X	Input variables regression model	-

1 Introduction

Researchers at the TU/e are working on metal fuels as a promising and sustainable alternative to fossil fuels, to prevent carbon emissions and avert climate change. During the iron cycle, iron powder is burnt and energy is released, leaving iron oxide as a combustion product. This can later be reduced back into iron powder, and by doing so closing the iron cycle. The main reason to use the iron cycle over alternative energy carriers is that the energy is carbon-free. Furthermore, the iron oxide can easily be reduced back to iron powder and stored when excessive green energy is available, which is a great advantage over batteries. Iron was chosen since it is an abundant metal, widely used for all kinds of applications [OpenWebcast, 2016].

During the research into the specific iron combustion process, an essential part is investigating the combustion products. This includes iron oxide, but could also contain unburned iron powder due to a lack of oxygen during combustion. Currently, cyclones are used in the lab to capture the particles from the exhaust airflow of iron burners. One of these cyclones is the Stairmand cyclone, which is a common type of cyclone, known for its high separation efficiency [Gopani and Bhargava, 2011]. It is however uncertain what the exact efficiency of this cyclone is, and if it yields reliable samples. Another problem with the existing Stairmand cyclone is the large pressure loss, which hinders the exhaust air flow of the iron burner. The goal of this report is to design a new cyclone that reduces the pressure drop, whilst maintaining or improving the particle separation efficiency.

This report first studies existing research in cyclone technology, since a lot of research has already been done to find expressions for the characteristics of cyclones. Three of the most important factors in the design of a cyclone are efficiency, pressure loss, and gas flow rate [Magoss et al., 2022]. These characteristics all depend on the design dimensions of the cyclone. Often this research is based on CFD simulations [Brar, 2018].
Next, this research is used to design a new cyclone specifically for filtering the exhaust gasses of the iron burners. For this, a numerical model is used, which is based on theoretical equations and CFD simulations.
The existing Stairmand cyclone and the newly designed cyclone will be tested for pressure drop during experiments. This can be used to verify the numerical model. Based on the results of the numerical model and the experiments, advice will be given for further research on the separation efficiency of the cyclone.

2 Cyclone Theory

In this section, the theory of the cyclone will be discussed. This includes the dimensions and ratios used to describe a cyclone, the pressure drop in a cyclone, and the cut-off diameter of the particles. Furthermore, also the selection of an appropriate pump and information about the iron powder is presented.

2.1 Design Parameters

There are two main types of cyclones with different designs. One has a tangential inflow direction, while the other has an axial inflow direction, see Figure 2.1. In an axial type cyclone, the dirty air enters from the top, and is brought into a swirling motion by so-called 'swirl vanes'. In a tangential type, the swirling flow of the air is caused by the location of the in-flowing air. The tangential velocity of the incoming air in an axial cyclone is lower, which reduces the separation efficiency. Currently, tangential cyclones are in use to separate iron powder due to their higher separation efficiency. This report focuses on tangential cyclones.

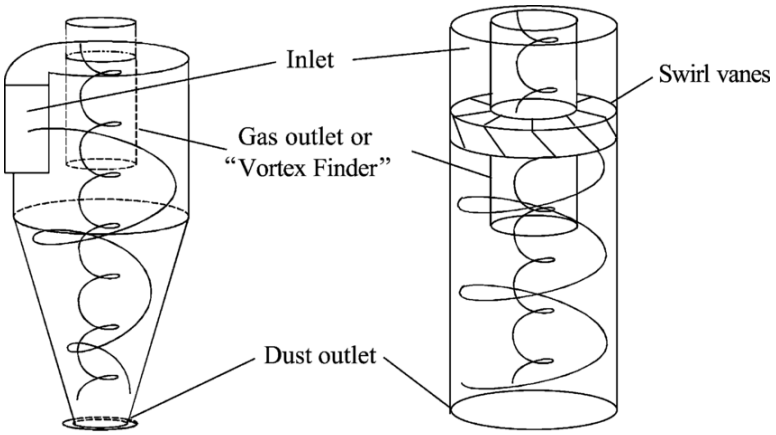

Figure 2.1: The differences between tangential inflow cyclone (left) and axial inflow cyclone (right) are the air inlet and swirl vanes. [Peng et al., 2002].

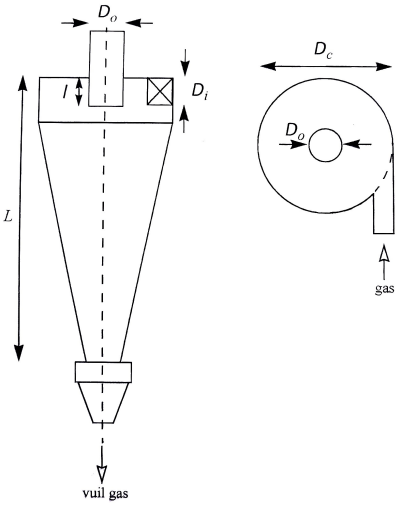

Figure 2.2: General dimensions of a tangential cyclone [van Esch, 2018]

In Figure 2.2 the general dimensions of a tangential cyclone are given. These are used throughout this report to indicate the dimensions of certain parts of the cyclone. D_c is the inner diameter of the top of the cyclone. D_o and D_i are the inner diameters of the exit and the inlet of the turbine respectively. L is the total inner height of the cyclone, and small l is the height of the outlet within the cyclone. Lastly, the cone angle is the angle of the tapered section of the cyclone.
In the calculations and design of a cyclone often ratios are used to describe the geometry of the cyclone. Only one of the dimensions thus has to be known. The dimension ratios of two common cyclones types are given in Table 2.1.

Type	D_i/D_c	D_o/D_c	l/D_c	L/D_c	Cone angle
Rietema	0.28	0.34	0.4	5	20
Existing (Stairmand)	0.167	0.20	0.50	4	7.125

Table 2.1: Dimension ratios of several cyclones [van Esch, 2018], [Gopani and Bhargava, 2011]

2.2 Air Flow and Cut-Off Diameter

The airflow in the cyclone follows a circular path due to the design of the cyclone. Due to the path centrifugal forces cause the heavier particles to move to the cyclone's wall. Because of the no-slip boundary

condition, the airspeed is zero at the wall, allowing the particles to move down towards the dirt collector close to the wall. Figure 2.3 clearly illustrates this flow.

$$v_{r,e} = \frac{Q}{2\pi r(L-l)} \tag{2.1}$$

The radial velocity is pointing inward, and the average velocity can be estimated by the flow rate Q divided by the area of the cylinder $2\pi r(L-l)$ since all flow must pass through this area in order to reach the exit, as shown in Equation 2.1. In this equation, r is the radius of the vortex finder ($D_o/2$) and $L-l$ is the height between the vortex finder and the bottom of the cyclone.

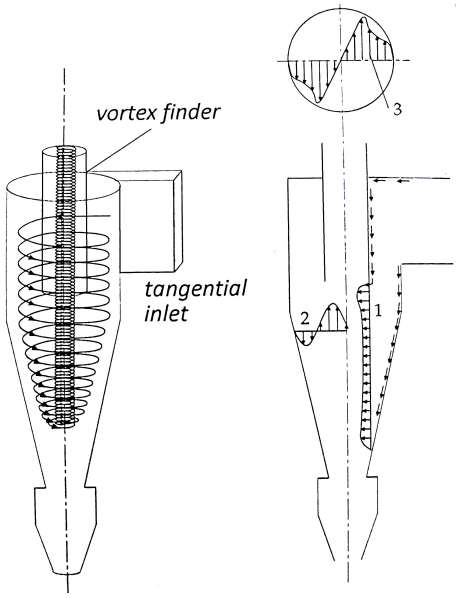

Figure 2.3: Air flow in cyclone with velocity vectors in radial (1), axial (2) and tangential (3) direction [van Esch, 2018]

Three forces act on the particles. These are the centrifugal force (Equation 2.2), the buoyancy force (Equation 2.3), and the resistance force due to air resistance (Equation 2.4). These all act in the radial direction. Only the centrifugal force acts in the outward direction. Because of this, it must hold that $F_c = F_d + F_{buo}$ for a steady particle in the flow. In the List of Symbols, the meaning of the symbols is given.

$$F_c = m_p \frac{v_\theta^2}{r} \tag{2.2}$$

$$F_{buo} = m_G \frac{v_\theta^2}{r} \tag{2.3}$$

$$F_d = C_D \frac{\pi}{4} d_p^2 \frac{1}{2} \rho_G v_{TC}^2 \tag{2.4}$$

In Appendix A.1, the three above equations are processed to form an expression for the cut-off diameter, shown in Equation 2.5. For this four assumptions are used. These are shown below:

- The Reynolds number in the radial direction is smaller than 1, for which it should hold that the radial velocity is smaller than 14 m/s. This way the friction coefficient C_d can be computed using the equation $C_d = 24/\mathrm{Re}$
- The tangential velocity is a free vortex (the further from the center, the lower the tangential velocity).
- The radial velocity is constant over the height of the cyclone at radius $D_0/2$.
- The radius at which the cut-off point of particles (50% separation) occurs is where the axial air velocity is zero.

$$d_{p,50\%} = \sqrt{\frac{36(D_o/2D_c)^2(D_i/D_c)^4}{\pi((L-l)/D_c)} \frac{\mu D_c^3}{(\rho_p - \rho_G)Q}} = \sqrt{\frac{9D_0^2 D_i^4}{\pi(L-l)D_c^2} \frac{\mu}{(\rho_p - \rho_G)Q}} \tag{2.5}$$

From Equation 2.5, it can be concluded that the particle cut-off diameter depends on multiple design ratios, as well as the overall scale of the cyclone, the flow rate, and particle density. To lower the cut-off diameter, and thus increase the cyclone efficiency, a higher flow rate or smaller cyclone can be used. The cyclone efficiency is defined as the percentage of mass which is captured by the cyclone for a given particle diameter. It must be noted that for higher gas temperatures, the viscosity increases, leading to a lower cyclone efficiency. For air at 500 °C, the cut-off diameter increases with a factor $\sqrt{2}$ compared to room temperature (Appendix A.5). Also, due to the assumptions, this equation should only be used as a correlation and approximation.

The cut-off diameter indicates the particle diameter at which 50 percent of the particles are separated and the other 50 percent is passed through the cyclone. To determine for which particle diameter the efficiency is higher than some set threshold, use can be made of a plot shown in Figure 2.4.
As an example from data of [Huang et al., 2018], the cyclone in this figure has a cut-off diameter of about 1.1 micrometers. For a particle of 2 micrometers, the efficiency is over 95%, and for a particle of 3 micrometers the efficiency approaches 100%.

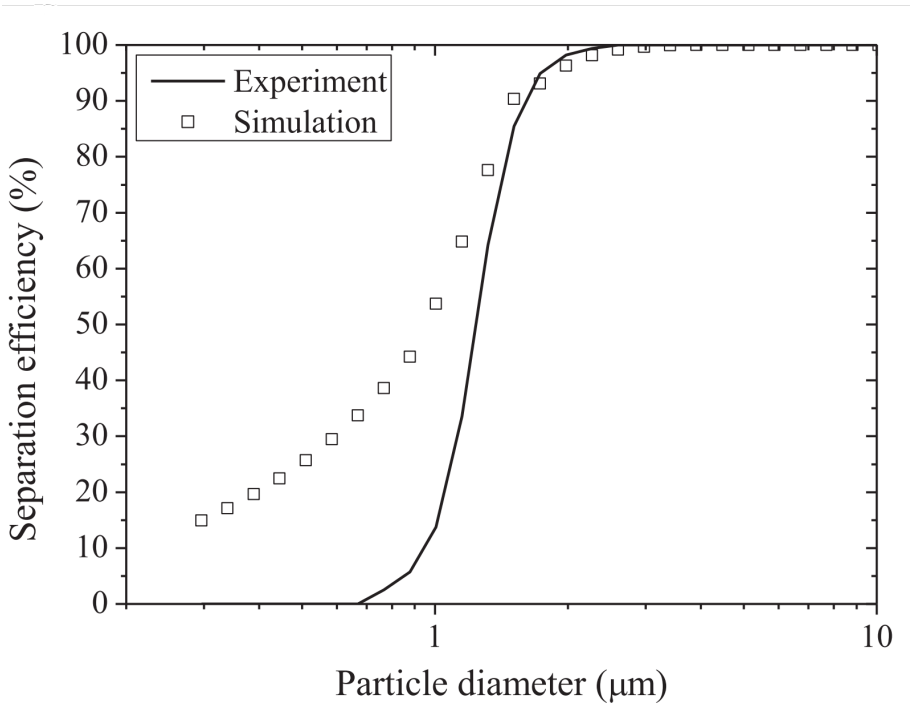

Figure 2.4: Seperation efficiency of a cyclone as a function of the particle diameter [Huang et al., 2018]

By adjusting variables like the scale of the cyclone or flow rate, the line in the graph can be shifted to the left or right, according to Equation 2.5. The steepness of the line indicates how quickly the efficiency increases dependant on the particle size. The steepness depends on several design factors, and will not be further discussed in this report [Huang et al., 2018].

2.3 Pressure Loss

An important factor in the performance of a cyclone is the pressure drop that occurs. Several expressions are found in the literature, all based on slightly different methods and assumptions. Below two of these expressions will be shown and compared.

The first equation for the pressure drop in a cyclone is by Rietema [van Esch, 2018]. This equation is based on the pressure drop in a pipe, and is shown in Equation 2.6. The corresponding Reynolds number and cyclone velocity are shown in Equation 2.7 and 2.8.

$$\Delta p = K\, Re^n \cdot \frac{1}{2}\,\rho_G\, v_c^2 \quad (2.6) \qquad Re = \frac{\rho_G\, v_c\, D_c}{\mu} \quad (2.7) \qquad v_c = \frac{4\,Q}{\pi\, D_c^2} \quad (2.8)$$

In this equation, K is a scalar which influences the overall pressure drop, whilst n indicates if pressure drop occurs for low or high flow rates. The constants K and n depend on the design of the cyclone, and are determined experimentally. In Table 2.2, some typical values for K and n are shown for well-known cyclone designs.

Cyclone type	**K [-]**	**n [-]**
Rietema	316	0.134
Bradley	446.5	0.323
Mozley-1	6381	0
Warman model R	2.618	0.8

Table 2.2: Typical values for K and n for well-known cyclone designs [van Esch, 2018]

A second equation for the pressure drop, developed by [Chen and Shi, 2007], is a lot more complex and consists of 4 separate pressure loss equations, based on theoretical knowledge. The first is the pressure loss due to expansion at the inlet of the cyclone. The second is the compression losses at the outlet. The third and fourth are swirling and gas energy dissipation losses. The total pressure drop can be calculated by the sum of the four individual equations, as shown in Equations 2.9 - 2.13. More information about the meaning of the variables can be found in the List of Symbols.

$$\Delta p = \Delta P_1 + \Delta P_2 + \Delta P_3 + \Delta P_4 \quad (2.9)$$

$$\Delta P_1 = \left(1 - \frac{2\,k_i\,\tilde{b}}{1 + 1.33\,\tilde{b} - \tilde{d}_r}\right)^2 \frac{\rho_g\, V_i^2}{2} \quad (2.10)$$

$$\Delta P_2 = 4.5 \frac{(1 - 3\,\tilde{d}_r^2)}{K_A^2}\,\frac{\rho_g\, V_i^2}{2} \quad (2.11)$$

$$\Delta P_3 = 1.11\, f_0\, K_A\, \tilde{F}_s\, \tilde{V}_{\theta\,w}^3\, \tilde{d}_r^{-1.5 n_s}\, \frac{\rho_g\, V_i^2}{2} \quad (2.12)$$

$$\Delta P_4 = \frac{\rho_g}{2}(V_\theta^2 + V_{ze}^2) \quad (2.13)$$

In all of the equations above a factor $\frac{\rho_g V^2}{2}$ is present, only with a varying subscript for the velocity. This is multiplied by several constants which depend on the cyclone design and materials.

The above pressure drop expressions from Rietema [van Esch, 2018] and [Chen and Shi, 2007] are similar, in that the velocity squared is multiplied by mostly constants. Due to the simplicity of the Rietema equation and the fact that this equation is easier to implement in practical experiments, this will be used for the remainder of this report.

2.4 Pump Selection

For the cyclone to work in its optimal condition, a steady and controllable airflow is required. Based on the pressure drop and cut-off diameter a flow rate is chosen. To achieve this flow rate, a pump should be chosen with the same head as the cyclone and hoses for a set flow rate. The head is defined as the maximum height a pump can push a fluid or gas in the vertical direction. This is usually highest for a near-zero flow rate. A simple valve or MFC can be used to control the flow rate.

For the selection of a suitable pump, use can be made of a head vs flow rate graph. In such a graph, the cyclone and piping head are roughly a second-order polynomial, which starts at the origin. The head of the pump can be approximated by a polynomial flipped around the x-axis, which starts at a head H_0 for zero flow rate. An example of such a graph can be seen in Figure 2.5, where it is clear that the pump selection is important to obtain the desired flow rate.

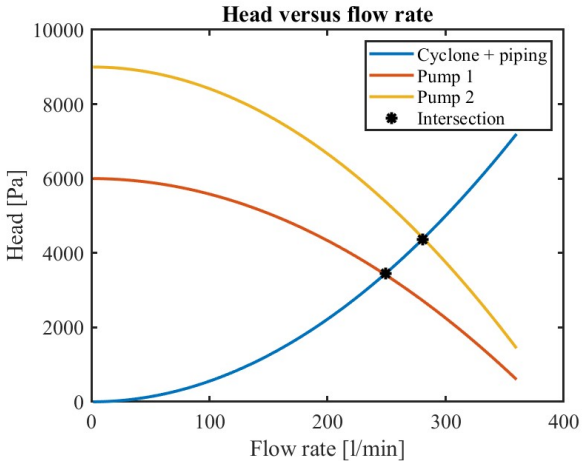

Figure 2.5: Example of head versus flow rate graph

2.5 Iron Powder

The size of the particles has a large influence on the separation efficiency of a cyclone, where larger particles are more easily filtered. During iron powder experiments at the TU/e, often powder with a particle diameter distribution between 5 to 9 μm is used. After combustion, iron oxide occurs, according to Equation 2.14.

$$4Fe + 3O_2 \rightarrow 2Fe_2O_3 \tag{2.14}$$

In the paper of [Buchheiser et al., 2023], it was found that the particle size of the iron oxide powder is larger compared to the iron powder. In his research, iron powder with a size of 5.67 ± 0.45 μm was burnt, resulting in iron oxide powder with a size of 9.78 ± 0.13 μm. This is also shown in Figure 2.6, where the x-axis indicates the fuel-air equivalence ratio, and the y-axis the particle diameter. From this, it can be concluded that the separation efficiency of the iron oxide powder will be higher than the unburnt iron powder.

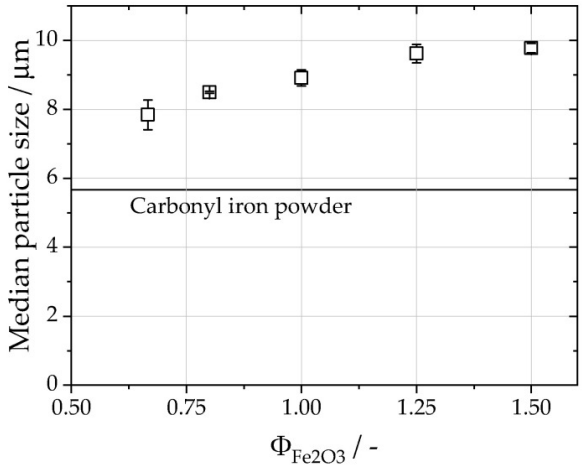

Figure 2.6: Iron oxide powder diameter as a function of the fuel to air ratio, with iron powder of 5.67 [Buchheiser et al., 2023]

3 Optimizing Cyclone

In this section, the optimization of the existing cyclone will be discussed, resulting in the design of a new cyclone. This will involve the cyclone theory as discussed in section 2, as well as a regression model developed by Brar [Bronkhorst, 2023].
For future referencing of the new and existing cyclone, configuration numbers are given, as shown in Table 3.1. Configuration 1 is the existing cyclone, which was built before this project. Configuration 2 is the new cyclone, is designed in this section. Since the cyclone parts are made interchangeable, configuration 3 is the new cyclone top combined with the existing main body, and configuration 4 is the old top and new body.

Configuration	**Top**	**Main body**
Conf 1	Existing	Existing
Conf 2	New	New
Conf 3	New	Existing
Conf 4	Existing	New

Table 3.1: Cyclone configuration numbers; The new cyclone is developed in this section.

3.1 Existing Cyclone

The new cyclone which is designed in this section has to be an improvement compared to the older cyclone. For this, it is important to take a look at the existing cyclone and see why the requirement for the pressure drop is not met.
In Figure 3.1a, the technical drawing of the current cyclone is shown. The normalized dimensions are given in Table 3.2, based on Figure 2.2. The values of a and b are the height and width of the rectangular-shaped inlet. The value of l indicates the length of the vortex-finder, which is connected to the top of the cyclone, and guides the airflow to the exit. The value H is the height of the cylinder in the cyclone. These ratios are all dependent on D, which is a value for the scale of the cyclone. The dimensionless ratio D_c/D is used to change the width of the cyclone, independent of the the other dimensions. For the existing cyclone, the ratio D_c/D is 1, so $D_c = D = 60\ mm$. For the new cyclone, the ratio D_c/D is 1.5 and the value of D is 43.3, resulting in a cyclone diameter of $43.3 \times 1.5 = 65\ mm$.

Type	a/D	b/D	D_o/D	l/D	L/D	H/D	D_c/D	Cone angle [°]	D [mm]
Existing (Conf 1)	0.5	0.2	0.5	0.5	4	1.5	1	7.125	60
New (Conf 2)	0.5	0.2	0.66	0.5	4	2	1.5	13.9	43.3
Conf 3	0.5	0.2	0.48	0.36	4	1.5	1	7.125	60
Conf 4	0.5	0.2	0.69	0.69	4	2	1.5	13.9	43.3

Table 3.2: Dimension ratios of the existing cyclone and new cyclone, as well as for configuration 3 and 4, corresponding to Table 3.1.

3.2 Requirements

During iron powder research, a cyclone is used to extract the iron oxide particles from the exhaust gasses of an iron burner. The experimental setup used for these experiments makes use of a vacuum or other type of extraction device to capture the particles. These devices create air flow based on lower air pressures. This limits the maximum pressure difference to 1 bar since the burner is placed at ambient pressure. For a flow rate required for the cyclone to work, the maximum pressure difference a vacuum can generate strongly decreases. For this reason, the pressure drop in the cyclone should be reduced.
The cut-off diameter of the cyclone may not increase, since this would lead to a lower separation efficiency.

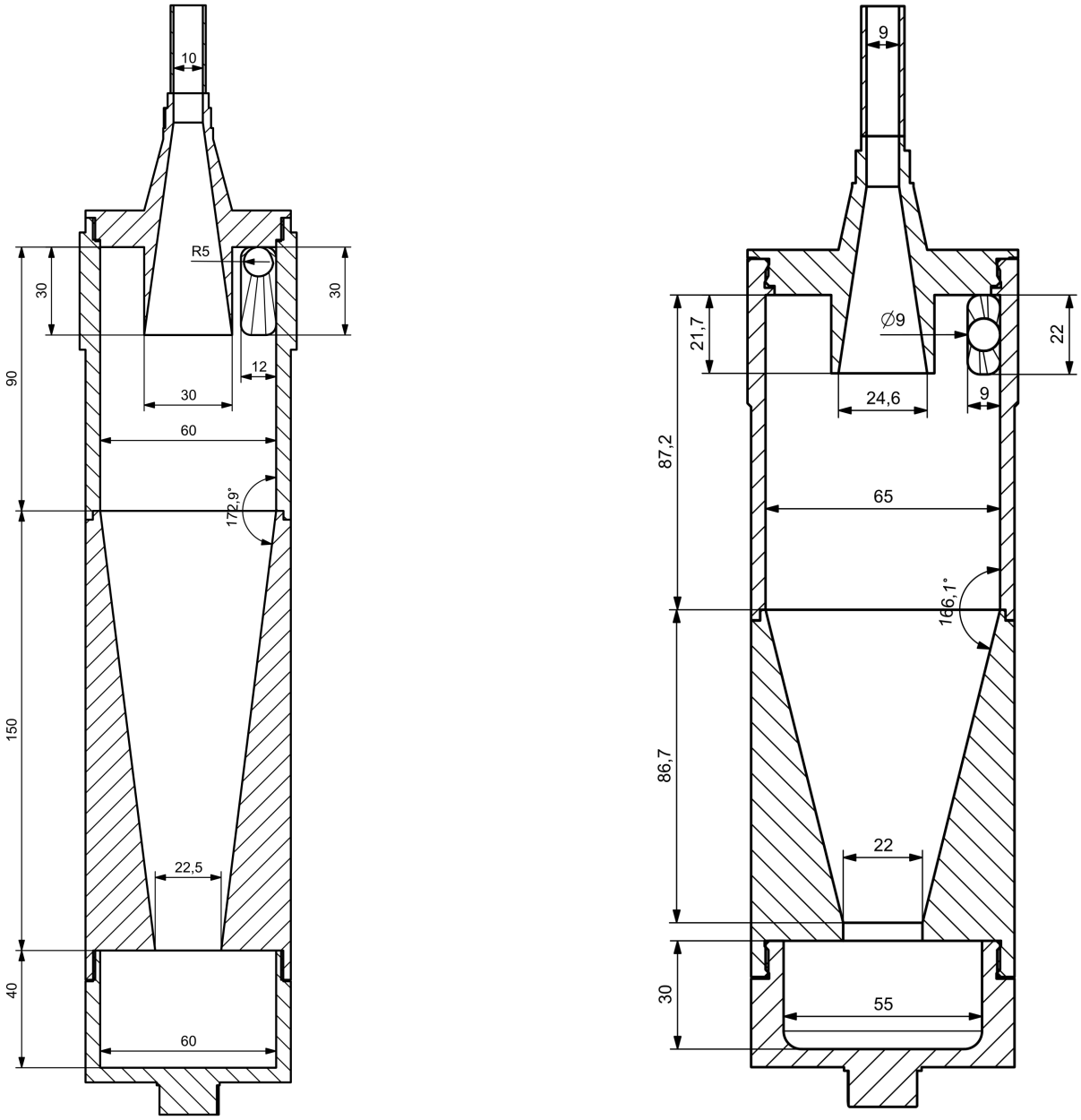

(a) Existing cyclone **(b)** New cyclone

Figure 3.1: Technical drawings of the cyclones

3.3 Modeling Optimal Design Parameters

To find the best cyclone parameters for the requirements, two separate but interconnected models are used. The first focuses on the design dimension ratios of the cyclone, and its effect on the cut-off diameter and pressure drop. The second part is the effects of the airflow rate and overall cyclone size on the particle cut-off diameter and pressure drop in the cyclone. These will then be combined into a final cyclone design, which will be further tested during the experiment to verify the models.

3.3.1 Cyclone Dimension Ratios

Several design parameters could be tested using the regression model of Brar [Brar, 2018]. This model was made by repeating CFD simulations of different cyclone designs. Using this data a regression model could be made, which allows for predictions of pressure drop and cut-off diameter for given dimension ratios.

$$Y = \beta_0 + \sum_{n=1}^{k} \beta_i X_i + \sum_{n=1}^{k} \beta_{ii} X_i^2 + \sum_{i<j} \beta_{ij} X_i X_j + \epsilon \tag{3.1}$$

In Equation 3.1 the formula for the regression model is shown, and the coefficients are in Table B.2. In Brar's simulations, the inlet velocity was constant with a value of 16.1 meters per second. The flow rate is the inlet area multiplied by the velocity. The value D was constant at 0.29 m. Furthermore, the viscosity of the air was 20×10^{-6} N s/m^2, a temperature of 23 degrees Celsius, a powder density of 2700 kg/m^3, and a particle diameter between 0.3 and 6.8 micrometers.
In his paper [Brar, 2018], Brar found the optimal design ratios for a cyclone with a low cut-off diameter and low-pressure drop. These ratios are used in the new cyclone and can be seen in Table 3.2 for configuration 2 (Conf 2).
To calculate the pressure drop using the regression model for the existing and new cyclone, with a diameter of 60 or 65 mm, use can be made of Equation 2.6 and Equations 3.2 - 3.4.

$$Q = v_{inlet} * A_{inlet} = 16.1\, a\, b\, D^2 \tag{3.2}$$

$$v_c = \frac{4Q}{\pi D^2} = \frac{64.4\, a\, b}{\pi} \cdot \left(\frac{D}{D_c}\right)^2 \tag{3.3}$$

$$Re = \frac{\rho v_c D_c}{\mu} = \frac{64.4\, \rho\, a\, b\, D}{\mu} \cdot \frac{D}{D_c} \tag{3.4}$$

From the aforementioned four equations, it can be seen that the velocity in the cyclone v_c does not change when the overall scale is changed since the flow rate is a quadratic function of the cyclone diameter and the ratio D_c/D is constant. The Reynolds number does change linearly with the value of D. Depending on the value of n (positive or negative) in Equation 2.6 the pressure drop increases or decreases for a different cyclone scale.

The same approach is used to apply a correction factor for the particle cut-off diameter using Equation 2.5. When all constants (ratios) are removed from the equation, one ends up with the following expression, which can be used to determine the ratio of the cut-off diameter without requiring all variables:

$$d_{p,50\%} = \sqrt{\frac{D_c^3}{Q}} \tag{3.5}$$

Since Q depends quadratically on the cyclone diameter, the ratio between the cut-off diameter for different cyclone scales is a function of the square root of the diameter. This means that for a smaller cyclone, the cut-off diameter also decreases.

By implementing the regression model, the above four equations, and the constants K and n in Equation 2.6 (determined experimentally in section 4) the theoretical pressure drop can be calculated. Using Matlab (code in Appendix B.3), the pressure drop and cut-off diameter are computed for the four cyclone configurations, with corrections for the different scale cyclones. The results of this can be seen in Table 3.3.

Configuration	Flow rate [l/min]	Pressure drop [Pa]	Cut-off diameter [μm]
Conf 1	348	482	0.727
Conf 2	191	247	0.571
Conf 3	348	547	0.681
Conf 4	191	220	0.614

Table 3.3: Results of the regression model, with dimensions from Table 3.2

Since the value of D (the scale of the cyclone) is smaller for the new cyclone, the flow rate is also smaller for the same inlet velocity. At the optimal flow rate, the pressure drop of configurations 2 and 4 (new body) is lower compared to configurations 1 and 3 (old body). The cut-off diameter for configuration 2 is the lowest, followed by configuration 4.
Using the n-values found during the experiments (section 4) and the computed pressure drop for a given flow rate, the K-values could be computed, and graphs can be made to show the theoretical pressure drop as a function of the flow rate. This is shown in Figure 3.2, with the values of K and n in Table 3.3. This graph shows that the pressure drop for a flow rate of 350 liters per minute is about twice as high for configurations 2 and 4, compared to configurations 1 and 3. This can be explained by the fact that the new cyclone is smaller, and is thus made for a lower flow rate. At these higher flow rates, the cut-off diameter decreases, leading to higher separation efficiencies.

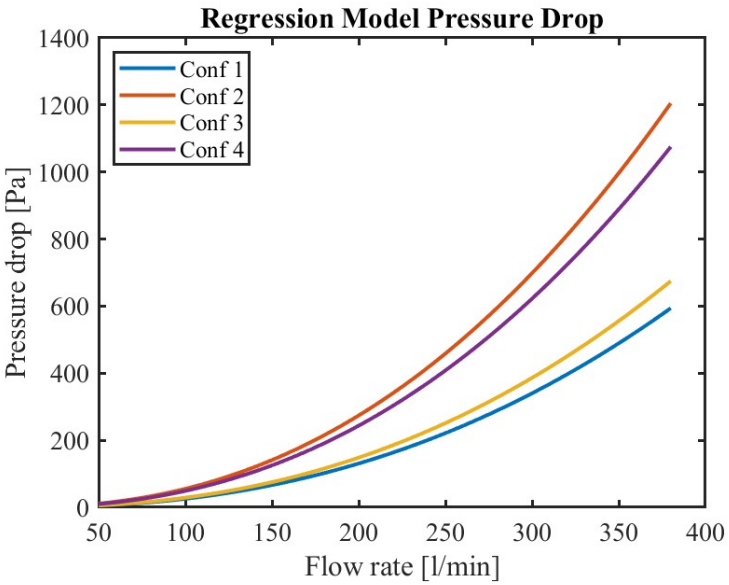

Figure 3.2: Pressure drop graph based on regression model for the four cyclone configurations, with dimensions from Table 3.2.

	K [-]	n [-]
Conf 1	6.86	0.3583
Conf 2	31.34	0.3082
Conf 3	7.60	0.3610
Conf 4	26.58	0.3137

Figure 3.3: K and n values used in Figure 3.2. The n values are determined experimentally in section 4, and K is computed based on n and the regression model.

In Figure 3.4, a similar graph to Figure 3.2 is presented, where the scale (D) of the new and existing cyclone is the same at 60 mm (instead of 43.33 for configuration 2). This reveals that the pressure drop for the new cyclone is indeed lower (-50%) compared to the existing cyclone if they were the same size. Table 3.5, derived similarly as Table 3.3, shows that for an equal cyclone scale, the cut-off diameter is also lower for configuration 2 compared to configuration 1. If the results of the experiment in section 4 confirm the regression model is accurate, then the data in Figure 3.4 confirms a lower pressure drop of the new cyclone.

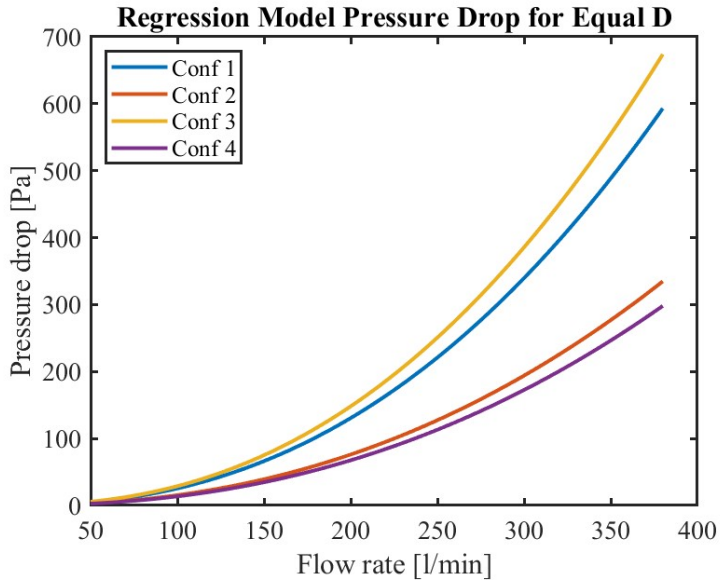

Figure 3.4: Pressure drop graph based on regression model for the four cyclone configurations, with equal value for D for all configurations.

	K [-]	**n [-]**
Conf 1	6.86	0.3583
Conf 2	35.37	0.3082
Conf 3	7.60	0.3610
Conf 4	29.99	0.3137

Figure 3.5: K and n values used in Figure 3.4. The n values are determined experimentally in section 4, and K is computed based on n and the regression model.

Configuration	**Flow rate [l/min]**	**Pressure drop [Pa]**	**Cut-off diameter [μm]**
Conf 1	348	482	0.727
Conf 2	348	273	0.672
Conf 3	348	547	0.681
Conf 4	348	243	0.722

Table 3.4: Results of the regression model where all four configurations have an equal D value of 60 mm.

3.3.2 Cyclone Size and Air Flow Rate

Based on the calculations in the previous chapters and the requirements of the new cyclone a model can be made to find the correct design parameters. The most important factors are the pressure loss, cyclone diameter, and the cut-off particle diameter. Implementing the formulas for the pressure drop and cut-off diameter into a Matlab script (code in subsection B.4) results in two different plots, which can be seen in Figures 3.6 and 3.7. These graphs show the relationship between flow rate and cyclone size and the cut-off diameter and pressure loss for an arbitrary cyclone. From these graphs, it can be concluded that both a higher flow rate and a smaller cyclone result in a lower cut-off diameter, which in turn results in a higher separation efficiency of the iron powder.
However, besides a high separation efficiency, a small cyclone or high flow rate also results in a higher pressure drop. To find the optimal values for the cyclone size and air flow rate, the requirements and physical limitations have to be taken into account.

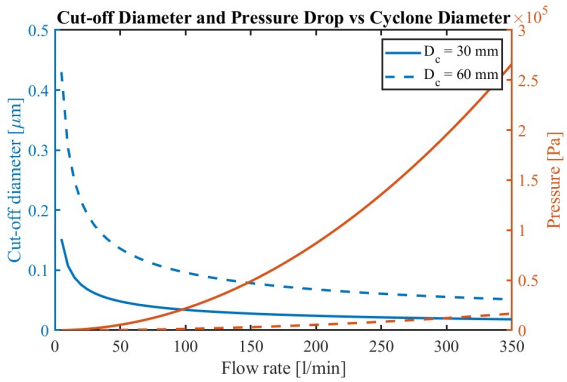

Figure 3.6: Cut-off particle diameter as a function of flow rate

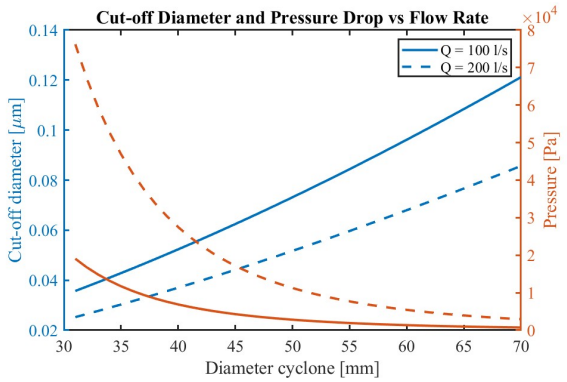

Figure 3.7: Cut-off particle diameter as a function of cyclone size

3.4 New Cyclone Design

Based on the calculations in this chapter, a new cyclone was developed. This uses the design ratios as shown for configuration 2 in Table 3.2. To be able to test multiple configurations of the cyclones, with for example a new top part, on the existing body, it was chosen to use the same thread (M65x1.5) on both cyclones, making the parts interchangeable. This set the diameter of the new cyclone D_c to 65 mm, which is slightly wider compared to the existing cyclone. The technical drawing is shown in Figure 3.1b. The main differences between the new and existing cyclones are the width and the inner shape of the cyclone. Where the existing cyclone has an angle of about 7 degrees, the new cyclone has an angle of almost 14 degrees. Furthermore, the ratio between the cylindrical-shaped section and the cone-shaped section is different for the new cyclone. This should lead to more clustering (agglomeration) of particles, leading to larger particles and thus higher separation efficiencies [Alves et al., 2015].

It should be noted that the new cyclone should be considered a 'smaller scale' cyclone, meaning the flow rate is lower. Instead of sampling all exhaust gasses from a burner, only a part of the gasses should go through the cyclone. The rest of the combustion gasses should go straight to an appropriate air filter.

4 Pressure Drop Experiment

To verify the models used in section 3 experiments have to be performed. In this experiment, the existing and the new cyclone will be tested for pressure drop as a function of the airflow rate. Since the new cyclone is made with the same connections, it is also possible to test different configurations, like the inlet of the new cyclone with the outlet of the existing cyclone (Table 3.1). This gives more insights into where pressure differences occur.

4.1 Setup

The setup used during the experiments is schematically shown in Figure 4.8. The air supply is from a compressor in another room, with a pressure of over 6 bar, which can be closed off with a ball valve. Just after the air supply, a pressure regulator is added. This is set to approximately 5 bar. An air tank is used to make sure the air pressure to the second pressure regulator and the mass flow controller (MFC) is constant. The second pressure regulator is mainly used for testing the setup and is set to about 5 bar during the experiments.
The three most important items of the setup are found at the end. The first of these is a MFC. This digitally controlled MFC is used to precisely control the flow rate of the air going through the system. After the MFC the cyclone itself is connected using flexible hoses and push-in fittings. Using two tee-fittings, both inputs of the pressure differential sensor are connected just before and after the cyclone. This allows for the measurement of the pressure drop of the cyclone and the short pieces of tubing connected to it. Lastly, a short piece of hose is added after the second tee-fitting, which acts as the outlet of the system.

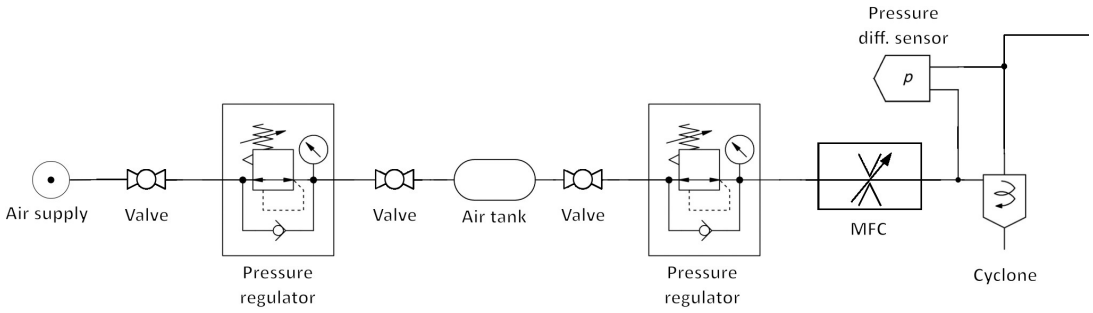

Figure 4.8: Schematic setup of the experiment

4.1.1 Setup Requirements

To successfully perform the experiments it is important that the setup meets certain requirements. For a wide range of measurements, a high flow rate is needed. To make sure this is possible most of the hoses have an outer diameter (OD) of 12 mm, and an inner diameter (ID) of 8 mm. This allows for flow rates over 300 l/min with a pressure drop of about two bar (subsection A.3).

Another important component is the MFC. This also has to be able to reach at least 250 l/s based on estimations of the flow rate. The best match available in the lab was an MFC with a rated flow rate of 300 l/min of methane. To convert the flow rate of methane to air, a conversion factor is used. This factor is about 0.77 and varies slightly based on the flow rate. Based on linear interpolation and the data (Figure B.1 [Bronkhorst, 2023]) provided by the manufacturer of the MFC, Bronkhorst, the conversion factors have been calculated and can be seen in Table B.1.
The input for the MFC control box is a percentage of the air flow rate. 100% air flow rate corresponds to about 76% flow rate of methane. For the experiments, an air flow range of 10 to 120 percent is used, which corresponds to 7.6 to 91% of methane. This is close to the high accuracy range of the MFC, which is between 10 and 90 percent of the rated flow rate [Bronkhorst, 2023].

The third and final component which has to be carefully chosen is the pressure differential sensor. The maximum pressure difference and the resolution are the two most important specifications of this sensor. Based on the model in the previous section, and the estimated pressure drop in hoses, the total pressure drop which would be measured is calculated (subsection A.2) to be about 0.2 bar.

Due to availability issues of pressure sensors with a range in the region of 0.5-1 bar, a pressure sensor with a range of 2 bar, and a resolution of 1 mbar is chosen. Due to the higher range the resolution is also higher, which could lead to less accurate measurements at low flow rates. A list of the items used during the experiment, including specifications can be seen in Table C.1.

4.2 Step Plan

To obtain the correct data from the experiment checklists must be followed to build the setup and to perform the experiment. Deviation from these checklists could lead to wrong measurements. In Appendix C.1, an elaborate building plan for the setup and preparation of the experiments is given.

To perform the experiments the step plan below should be followed, after completing the aforementioned steps.

1. Set the flow rate to 10%. After 20 seconds (subsection A.6), log the pressure drop reading in an Excel sheet.
2. Increase the flow rate with 5 percent, and repeat step 6 until a maximum flow rate of 120% is reached. Save the data.

To test the differences between the different cyclone configurations multiple experiments are performed. This is based on Table 4.1. First, the pressure drop in the hoses between the two tee connectors is tested (see **??**). Next, the three other cyclone configurations are tested. These can then be compared to the existing cyclone.

Experiment	**Cyclone**
1	12 mm hose
2	Conf 1
4	Conf 2
5	Conf 3
6	Conf 4

Table 4.1: Experiment configurations

4.3 Data Processing

The flow rate and pressure drop have been measured during the experiments with the different configurations according to Table 4.1. The results of the data should be the K and n values in Equation 2.6 for each of the four configurations. To retrieve the desired cyclone pressure loss data some processing has to be performed first.
The first step is to subtract the pressure losses which occur in the hoses and connections between the two tee connectors. The pipe losses are measured in experiment 1, where the cyclone was replaced by a 15 cm piece of 12 mm outer-diameter pipe, as shown in Figure 4.9. Using Equation 4.1 the pressure drop in the pipes is calculated. The values K_1 and n_1 are computed using the Matlab function "lsqcurvefit". This function is used to fit a curve or a mathematical model to a set of data points by minimizing the sum of squared differences between the observed and predicted values. The data points, in this case, are the pressure drop and flow rate, and the curve is Equation 2.6.

$$\Delta p_1(Q) = K_1 \, Re^{n_1} \cdot \frac{1}{2} \, \rho_G \, v^2 \tag{4.1}$$

$$\Delta p_{i,corrected}(Q) = \Delta p_i(Q) - \Delta p_1(Q) \qquad i \geq 2 \tag{4.2}$$

With the pressure drop in the pipes known, the pressure drop in the four cyclone configurations can be computed using Equation 4.2. Again using the "lsqcurvefit" function the K and n values for each of the four configurations can be computed using the corrected pressure drop. These can later be used to plot graphs of the pressure drop.
The R-squared value can be calculated to determine the quality of the fit (Equation A.14 - A.17).
The Matlab code used for fitting the data is given in Appendix B.5.

Figure 4.9: Hosing used during pipe pressure loss experiment

4.4 Results

In the results section, the experiment results are shown based on the measured setup, as shown in Table 4.1. First, the pressure drop in the hoses connected to the cyclone from experiment 1 is shown, since these are important for the data of the other experiments. Next, a comparison of experiments 2, 3, 4, and 5 is shown, to see how the pressure drop is influenced by the design of the cyclone.
A plot with the raw measured data can be seen in Figure C.1.

4.4.1 Experiment 1

In Figure 4.10, the experiment data is shown for the pressure drop in the pipes between the two pressure sensing positions. For an airflow rate of 360 liters per minute, the pressure drop is about 0.2 bar. This data is fitted to Equation 4.1, which resulted in $K_1 = 9059.1$ and $n_1 = -0.0331$.
The R squared value of the fit is 0.9987, which means the fitted curve closely resembles the measured data and allows it to be used to subtract the pipe losses from the measured data, leaving only the cyclone losses (Equation 4.2).

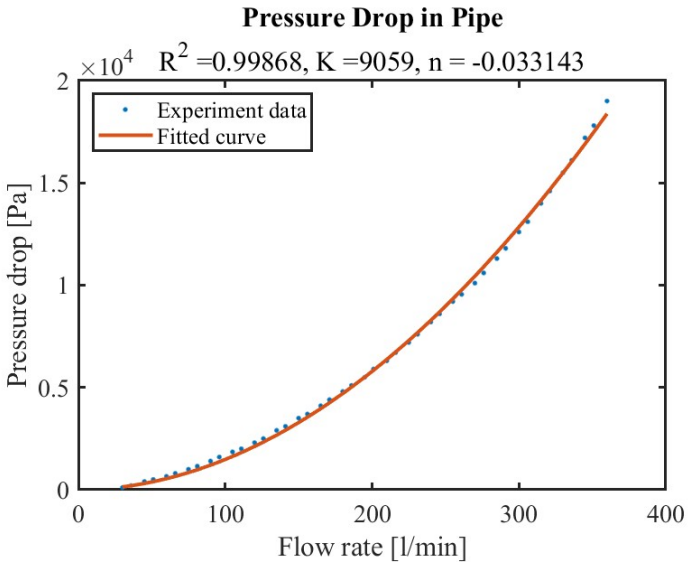

Figure 4.10: Experimental data of the pressure drop in the pipes and connectors.

4.4.2 Experiment 2, 3, 4 and 5

For each of the experiments 2 to 5, the piping losses are subtracted from the measured data. The resulting pressure drop is fitted to Equation 2.6. In Figure 4.11 the fitted data for each of the four cyclone configurations is shown. The fitted curves all have an R-squared value above 0.9964, which confirms a good fit for the measured data.
Table 4.2 shows the K and n values that are fitted to the data for the four cyclone configurations. Notable from this overview is that the n values are all in a small range, between 0.30 and 0.36. The K factors have a larger variation, from 160 to 680. Furthermore, configurations 1 and 3 (old main body) both have a low K and high n, whereas configurations 2 and 4 (new body) have a much higher K and lower n. This means the new main body of the cyclone has a higher pressure drop (K) but is less influenced by the flow rate compared to the old main body (n).

	Conf 1	**Conf 2**	**Conf 3**	**Conf 4**
K [-]	160.1576	678.0084	170.6526	598.4725
n [-]	0.3583	0.3082	0.3610	0.3137

Table 4.2: K and n values of cyclone configurations 1 to 4

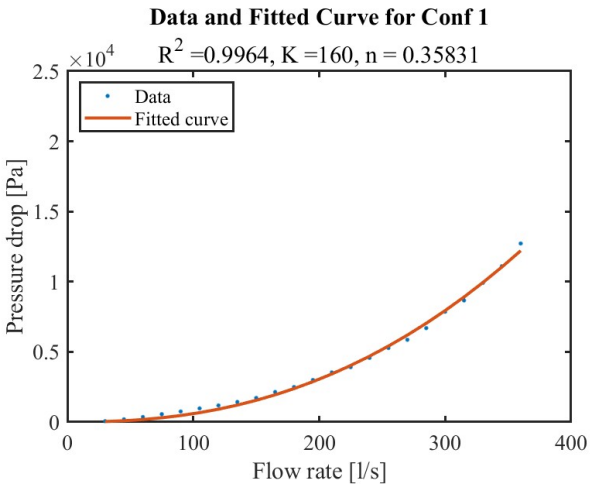

(a) Experiment 2

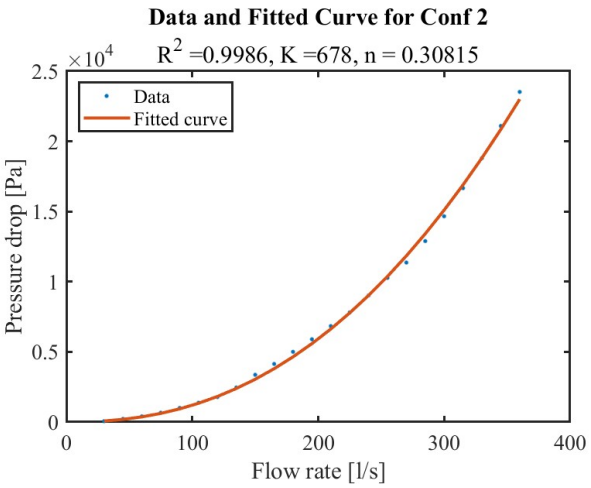

(b) Experiment 3

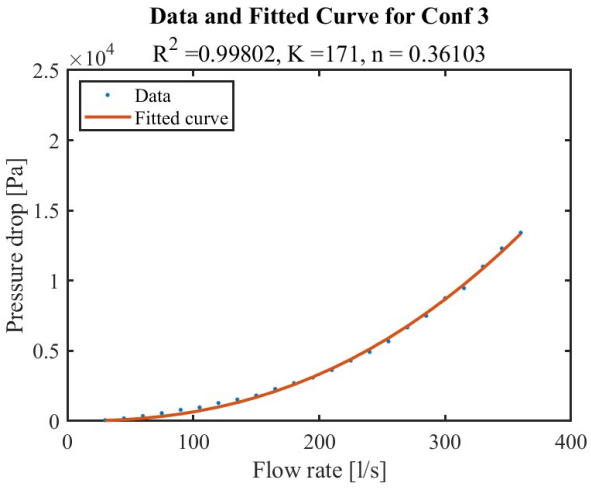

(c) Experiment 4

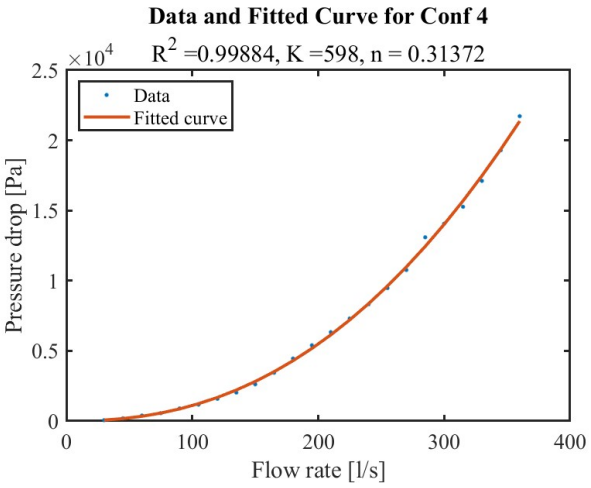

(d) Experiment 5

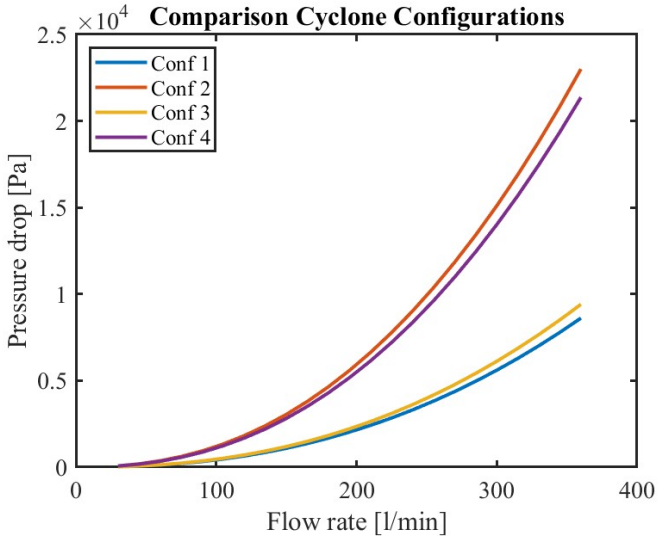

(e) Combined fitted curves experiments 2-5

Figure 4.11: Fitted data for experiments 2-5

4.5 Comparison Theoretical Model and Experiment

The experiment is performed to verify the theoretical model in section 3. In Figure 3.2, the resulting pressure drop versus flow rate is presented. In Figure 4.11e, the experimental pressure drop versus flow rate is presented for configurations 1 to 4. In Appendix B.6, the two aforementioned graphs are placed side by side, for an easy comparison. In both graphs, the order of the configurations is the same, where configuration 1 has the lowest pressure drop and configuration 2 the highest. Furthermore, configurations 1 and 3 are close together, as well as configurations 2 and 4. This is due to the same main body of the cyclone. This reveals that the shape of the body of the cyclone has a more profound effect on the pressure drop compared to the top of the cyclone.
In Figure 4.12, the existing (conf 1) and new (conf 2) cyclones are compared. Note that the y-axis is different. From this graph it can be concluded that the difference in pressure drop predicted by the regression model is larger then the measured difference during the experiment.

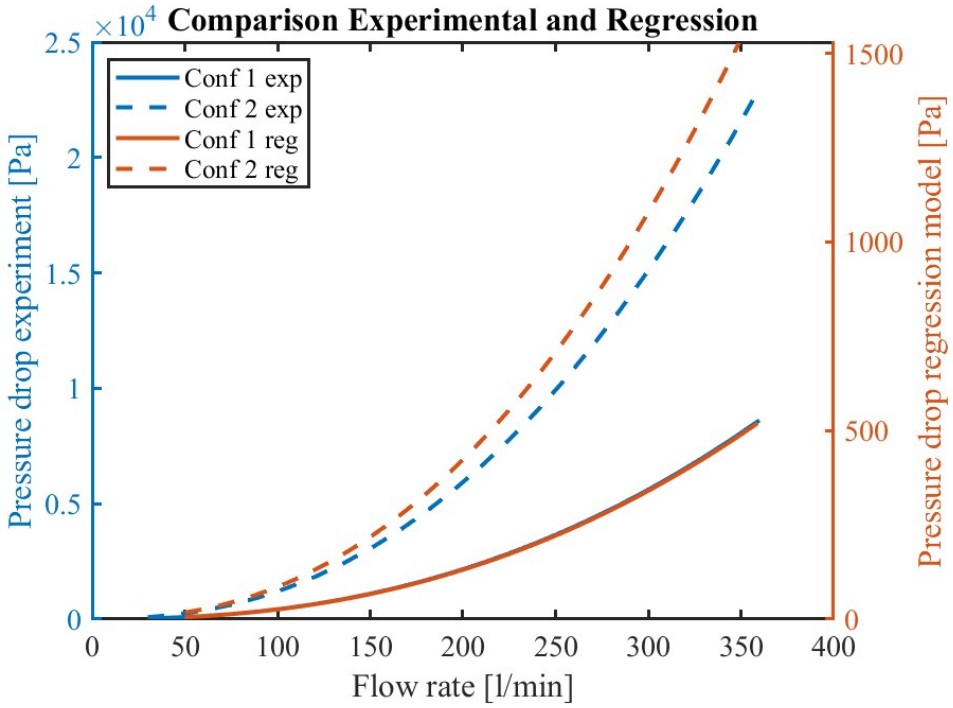

Figure 4.12: Comparison of the regression model and the experimental data for configurations 1 and 2

A difference between the model and the experiment is that a larger pressure difference occurs between configurations 1 & 3 and 2 & 4. This could be caused by the vortex finder. The new vortex finder has a constant wall thickness, whereas the existing vortex finder has a tapered edge, increasing the outlet side, and thus reducing the pressure drop. To improve the performance of the new cyclone the vortex finder could be made with a tapered edge, similar to the existing top.
Another important difference is the scale of the y-axis. The experimental pressure drop data is about a factor of 15 higher compared to the model. This is most likely caused by the losses in the pipes. The pipe losses were subtracted from the cyclone pressure drop (Equation 4.2). A possible explanation could be that the length of the pipe used during the hose pressure drop experiment was too short. If the K-value from the pipe losses is increased by a factor of 1.5, the differences between the regression model and experiment reduces to about a factor of 4. This could be an effect of the converging in- and outlet, which does not occur in the straight pipe. Further research is required to determine the cause of the difference in magnitude of the pressure drop.

5 Conclusion and Recommendations

In conclusion, this report has investigated a new cyclone design to sample iron (oxide) powder from an iron burner setup. The focus of this report is to reduce the pressure drop of the cyclone which is currently used in the lab, which is based on the Stairmand design.

First, an overview is given of the dimensions and common design of cyclones, including equations to calculate the pressure drop and particle cut-off diameter. Using a regression model developed by [Brar, 2018], the optimal design ratios were found, which were combined with a numerical model to end up with an improved cyclone. A new cyclone was built with these ratios, which was interchangeable with the existing cyclone, allowing for extensive testing of four different cyclone configurations.

The results of the pressure drop experiments of four different cyclone configurations proved the regression model for the pressure drop is valid under the assumption that the difference in magnitude of the pressure drop is caused by an incorrect measurement of the pipe pressure drop, as mentioned in section 4. From Figure 3.4, where the scale of the new cyclone was adjusted to 60 mm, it can be concluded that the new cyclone design reduced the pressure drop by about 50%. One small design change to further decrease the pressure drop of the new cyclone would be to taper the vortex finder.

5.1 Recommendations

Due to delays in the manufacturing of the new cyclone, the cyclones could not be tested with a dispersion system. This could have an effect on the pressure drop in a cyclone, as investigated by [Kumar and Jha, 2022]. In future studies, it would be beneficial to further investigate this effect. Furthermore, the separation efficiency and cut-off diameter should be investigated. The regression model in section 3 suggests the new cyclone has a slightly higher efficiency, but this should be verified experimentally. A third recommendation is to retest the pressure drop in the hose and to see its effect on the different magnitudes of the pressure drop between the regression model and the experiment.
A fourth recommendation to further study is the selection of a suitable pump (subsection 2.4) and, if the pressure drop is still too high, increase the diameter of the inlet and outlet hose connection.

Overall, this report provides valuable insights into the pressure drop of cyclones, which resulted in a new cyclone with a lower pressure drop. This information, combined with further research can be used to accurately sample iron powder using cyclones.

References

[Alves et al., 2015] Alves, A., Paiva, J., and Salcedo, R. (2015). Cyclone optimization including particle clustering. *Powder Technology*, 272:14–22.

[Brar, 2018] Brar, L. (2018). Application of response surface methodology to optimize the performance of cyclone separator using mathematical models and CFD simulations. *Materials Today: Proceedings*, 5:20426–20436.

[Bronkhorst, 2023] Bronkhorst (2023). GAS CONVERSION FACTOR CALCULATIONS.

[Buchheiser et al., 2023] Buchheiser, S., Deutschmann, M. P., Rhein, F., Allmang, A., Fedoryk, M., Stelzner, B., Harth, S., Trimis, D., and Nirschl, H. (2023). Particle and Phase Analysis of Combusted Iron Particles for Energy Storage and Release. *Materials*, 16(5).

[Chen and Shi, 2007] Chen, J. and Shi, M. (2007). A universal model to calculate cyclone pressure drop. *Powder Technology*, 171(3):184–191.

[Gopani and Bhargava, 2011] Gopani, N. and Bhargava, D. a. (2011). Design of High Efficiency Cyclone for Tiny Cement Industry. *International Journal of Environmental Science and Development*, 2:350–354.

[Huang et al., 2018] Huang, A. N., Ito, K., Fukasawa, T., Fukui, K., and Kuo, H. P. (2018). Effects of particle mass loading on the hydrodynamics and separation efficiency of a cyclone separator. *Journal of the Taiwan Institute of Chemical Engineers*, 90:61–67.

[Kumar and Jha, 2022] Kumar, V. and Jha, K. (2022). Effects of Mass-Loading on Performance of the Cyclone Separators. In Bhattacharyya, S., editor, *Applications of Computational Fluid Dynamics Simulation and Modeling*, page Ch. 12. IntechOpen, Rijeka.

[Magoss et al., 2022] Magoss, E., Sitkei, G., and Kocsis, Z. (2022). Separation of Particles from the Airflow. In *SpringerBriefs in Applied Sciences and Technology*, pages 59–82. Springer Science and Business Media Deutschland GmbH.

[OpenWebcast, 2016] OpenWebcast (2016). TU/e EnergyDays: Metal Fuels - 15 min.

[Peng et al., 2002] Peng, W., Hoffmann, A. C., Boot, P. J., Udding, A., Dries, H. W., Ekker, A., and Kater, J. (2002). Flow pattern in reverse-flow centrifugal separators. *Powder Technology*, 127(3):212–222.

[van Esch, 2018] van Esch, B. (2018). *Thermal and Fluid Engineering 4PC00.*

A Appendix A

A.1 Derivation Particle Diameter

Based on [van Esch, 2018].

$$F_c = m_p \frac{v_\theta^2}{r} \quad \text{(A.1)} \qquad F_{buo} = m_G \frac{v_\theta^2}{r} \quad \text{(A.2)} \qquad F_d = C_D \frac{\pi}{4} d_p^2 \frac{1}{2} \rho_G v_{TC}^2 \quad \text{(A.3)}$$

Rewriting this equation to the settling velocity gives:

$$v_{TC}^2 = \frac{8 v_\theta^2 (m_p - m_G)}{r C_D \pi d_p^2 \rho_G} \tag{A.4}$$

Using $m = \rho V = \rho \frac{\pi}{6} d_p^3$ this can be rewritten in terms of the densities of the gas and particle:

$$v_{TC}^2 = \frac{4 v_\theta^2 d_p (\rho_p - \rho_G)}{3 r C_d \rho_G} \tag{A.5}$$

Under the assumption that the reyonds number in radial direction is smaller than 1, C_D becomes $\frac{24}{Re} = \frac{24 \mu_g}{\rho_G v_{TC} d_p}$. Substituting this in the above equations gives the final expression for the settling velocity:

$$v_{TC} = \frac{(\rho_p - \rho_G) v_\theta^2 d_p^2}{18 r \mu_G} \tag{A.6}$$

The tangential velocity can be approximated by a free vortex flow. It then holds that $v_\theta r_e = c$ or $v_\theta = \frac{c}{r_e}$. Furthermore, it is assumed that the tangential velocity at radius $r = D_c/2$ is equal to $v_\theta = Q/A_{inlet}$. This can be combined into an equation for the tangential velocity as a function of the flow rate and the radius:

$$v_{\theta,r} = \frac{D_c Q}{2 A r_e} \tag{A.7}$$

The radial velocity can also be approximated by the assumption that the radial velocity is constant over the height of the cyclone $L - l$. The area the flow should pass through is the area of a cylinder at radius r_e, thus $A_c = 2\pi r_e (L - l)$. The radial velocity is the flow rate devided by the area:

$$v_{r,e} = \frac{Q}{2\pi r_e (L - l)} \tag{A.8}$$

v_{TC} and $v_{r,e}$ are the radial velocity of the particle and gas flow. If these are set equal to each other, and substituting the tangential flow velocity, the equation can be rewritten into the particle diameter:

$$d_p^2 = \frac{36 \mu r_e^2 A^2}{\pi (\rho_p - \rho_G) Q (L - l) D_c^2} \tag{A.9}$$

The particle diameter with a 50% change of being filtered is at a radius where the axial velocity is equal to zero. Larger and heavier particles will have a higher chance of being filtered at the same radius, because the centrifugal forces are larger. In figure 2.3 this is visualized. The zero velocity radius is assumed to be at half the diameter of the outlet since the flow within this radius will be upward towards the outlet.

The above equation can be rewritten in terms of the 50% seperation diameter and the design parameters, as mentioned in subsection 2.1. This results in the following formula:

$$d_{p,50\%} = \sqrt{\frac{36 (D_o/2D_c)^2 (D_i/D_c)^4}{\pi ((L - l)/D_c)} \frac{\mu D_c^3}{(\rho_p - \rho_G) Q}} = \sqrt{\frac{9 D_0^2 D_i^4}{\pi (L - l) D_c^2} \frac{\mu}{(\rho_p - \rho_G) Q}} \tag{A.10}$$

A.2 Expected Pressure Drop Cyclone Connections

$$Re = \frac{\rho * v * D}{\mu} = \frac{1.2 * 100 * 0.008}{18E - 6} \tag{A.11}$$

The given Reynolds number, combined with the roughness of the hoses ($\epsilon = 0.0015$), the friction factor f becomes 0.09 [van Esch, 2018].
With the T-connections and pipe couplings, a value of roughly 3 is obtained for K. The pressure drop in the piping and fittings between the pressure sensor locations is estimated using the formula below:

$$\Delta p = (f\frac{l}{D} + \sum K)\frac{1}{2}\rho v^2 \approx 0.18 \ bar \tag{A.12}$$

A.3 Pressure Drop Hoses

Assuming an inner diameter of 8 mm, length of 3 meters, friction factor of 0.09, and flow rate of 300 l/s, the pressure drop in the hoses is given below:

$$\Delta p = f\frac{L}{D} * \frac{1}{2}\rho v^2 = 2.04 \ bar \tag{A.13}$$

A.4 Calculation R^2

To quantify the quality of the fitted data the R-squared value is important. The close to 1, the better the fit. It can be calculated with the equations below:

$$y = \frac{1}{n}\sum_{i=1}^{n} y_i \quad \text{(A.14)} \qquad SS_{res} = \sum_i (y_i - f_i)^2 \quad \text{(A.15)} \qquad SS_{tot} = \sum_i (y_i - \bar{y})^2 \quad \text{(A.16)}$$

$$R^2 = 1 - \frac{SS_{res}}{SS_{tot}} \tag{A.17}$$

A.5 Separation Efficiency As a Function of Fime

The equation for particle cut-off diameter is given in Equation A.10. The viscosity of air at 20° is 18.24×10^{-6} N s/m^2, and 36.62×10^{-6} N s/m^2 for 500°. This is a factor 2 difference. Since the viscosity in the equation for the cut-off diameter is a square root, the cut-off diameter increases with a factor of $\sqrt{2}$ for air at 500° compared to air at room temperature.

A.6 MFC Reaction Time

To determine the time it takes for the MFC to settle at its given target flow rate, the flow rate is recorded as a function of time. The result can be seen in Figure A.1. From this graph, it can be concluded that the target flow rate is reached in about 10 seconds, with an error of 0.13 percent. Combined with about 10 seconds for the pressure sensor the total waiting time between adjusting the flow rate and the pressure difference read-off should be 20 seconds.

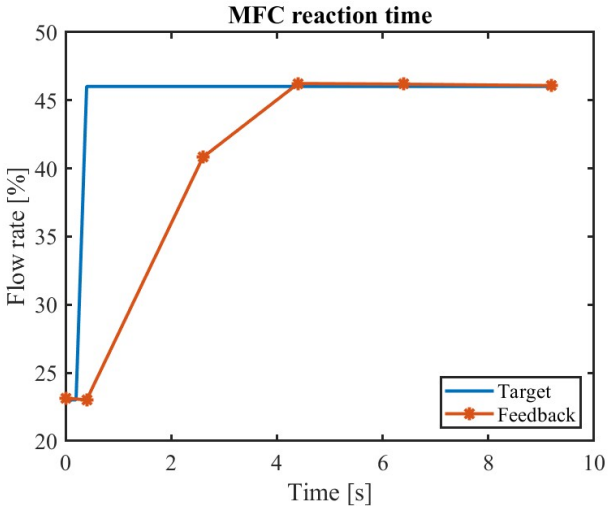

Figure A.1: Settling time MFC

B Appendix B

B.1 MFC Conversion Factor

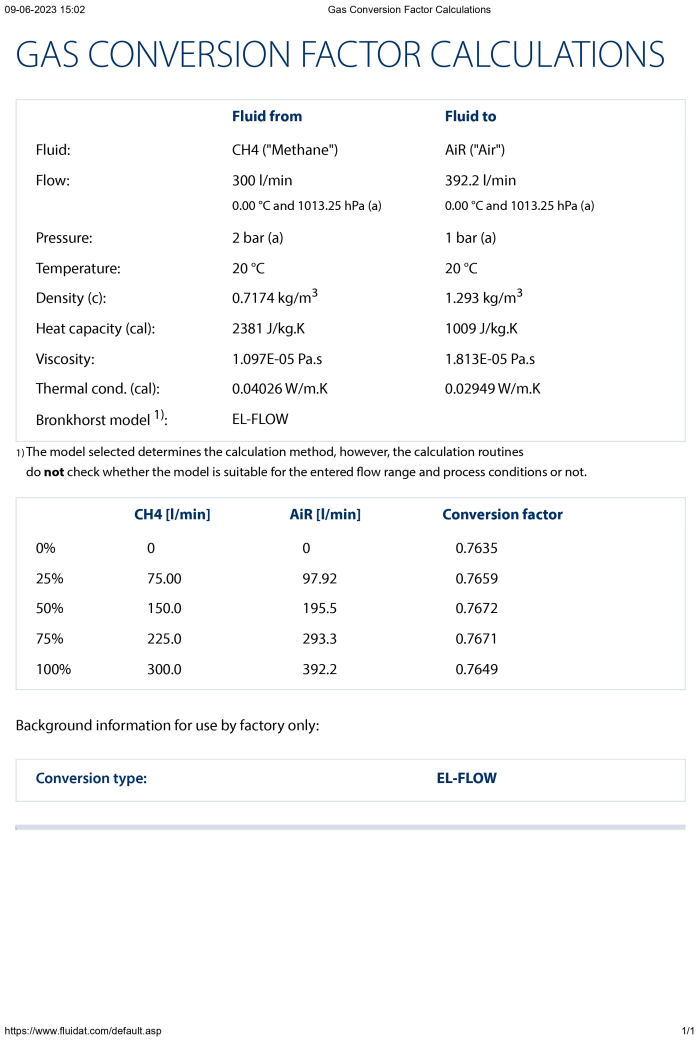

09-06-2023 15:02 Gas Conversion Factor Calculations

GAS CONVERSION FACTOR CALCULATIONS

	Fluid from	Fluid to
Fluid:	CH4 ("Methane")	AiR ("Air")
Flow:	300 l/min 0.00 °C and 1013.25 hPa (a)	392.2 l/min 0.00 °C and 1013.25 hPa (a)
Pressure:	2 bar (a)	1 bar (a)
Temperature:	20 °C	20 °C
Density (c):	0.7174 kg/m^3	1.293 kg/m^3
Heat capacity (cal):	2381 J/kg.K	1009 J/kg.K
Viscosity:	1.097E-05 Pa.s	1.813E-05 Pa.s
Thermal cond. (cal):	0.04026 W/m.K	0.02949 W/m.K
Bronkhorst model [1]:	EL-FLOW	

1) The model selected determines the calculation method, however, the calculation routines do **not** check whether the model is suitable for the entered flow range and process conditions or not.

	CH4 [l/min]	AiR [l/min]	Conversion factor
0%	0	0	0.7635
25%	75.00	97.92	0.7659
50%	150.0	195.5	0.7672
75%	225.0	293.3	0.7671
100%	300.0	392.2	0.7649

Background information for use by factory only:

Conversion type:	EL-FLOW

https://www.fluidat.com/default.asp 1/1

Figure B.1: MFC conversion factor data [Bronkhorst, 2023]

Flow rate percentage	0	10	20	30	40	50
Conversion factor	0.7635	0.7645	0.7654	0.7662	0.7669	0.7672
Flow rate percentage	60	70	80	90	100	
Conversion factor	0.7672	0.7671	0.7667	0.7658	0.7649	

Table B.1: Conversion factors MFC

B.2 Regression Model Coefficients

Term	Coefficient	P-value
β_0	5013.23	
Linear		
β_1	-14816.7	0.0000
β_2	-6.43083	0.1579
β_3	1347.92	0.0059
β_4	-664.304	0.0247
β_5	6.11325	0.2356
Quadratic		
β_{11}	10244.8	0.0000
β_{22}	-20.2634	0.7292
β_{33}	-247.601	0.3377
β_{44}	130.066	0.4295
β_{55}	-2.19246	0.9324
Interactive		
β_{12}	58.3531	0.6383
β_{13}	-580.251	0.1401
β_{14}	753.066	0.0470
β_{15}	37.0771	0.7172
β_{23}	-34.633	0.8263
β_{24}	-2.86083	0.9826
β_{25}	12.0614	0.7676
β_{34}	-5.12376	0.9845
β_{35}	-49.3167	0.5535
β_{45}	12.448	0.8464

(a) Pressure drop

Term	Coefficient	P-value
β_0	1.32318	
Linear		
β_1	4.99523	0.0000
β_2	0.0987341	0.0001
β_3	-2.24432	0.0000
β_4	-0.0903146	0.0492
β_5	0.0111183	0.1061
Quadratic		
β_{11}	-0.202652	0.1317
β_{22}	0.0822111	0.0445
β_{33}	0.988839	0.0022
β_{44}	0.0250071	0.7299
β_{55}	-0.000687999	0.9541
Interactive		
β_{12}	0.469605	0.0028
β_{13}	-2.06292	0.0006
β_{14}	0.222628	0.1281
β_{15}	0.00336809	0.9426
β_{23}	-0.203294	0.0559
β_{24}	0.0372547	0.5518
β_{25}	0.00498262	0.8318
β_{34}	-0.0208985	0.8639
β_{35}	0.0070748	0.8496
β_{45}	-0.0225044	0.4695

(b) Cut-off diameter

Input variable	
X_1	D_e/D
X_1	l/D
X_1	D_c/D
X_1	D_w/D
X_1	H/D

(c) Input

Table B.2: Regression coefficients for regression model

B.3 Matlab Code Regression Model

```
    clc, clear all, close all;

load("DesignParameters.mat")
n = [0.3583; 0.3082; 0.3610; 0.3137];

D_paper = 0.29;                                          % Diameter of
    cyclone in paper

v_in = 16.1;                                             % Inlet
    velocity [m/s]
A_in = input(:,7).*input(:,8)/1e6;      % Inlet area [m^2]
Q = v_in*A_in;                                           % Flow rate [m
    ^3/s]

D_c_K = input(:,3).*input(:,6)/1000;
D = input(:,6)/1000;
input = input(:,1:5);

%% Pressure drop
linear_p = [-14816.7; -6.43083; 1347.92; -664.304; 6.11325];
quad_p = [10244.8; -20.2634; -247.601; 130.066; -2.19246];
inter_p =[0       58.3531    -580.251     753.066     37.0771;
          0          0        -34.633    -2.86083    12.0614;
          0          0           0       -5.12376    -49.3167;
          0          0           0            0        12.448;
          0          0           0            0          0   ];

for i = 1:height(input)
        pressure(i) = input(i,1:5)*linear_p + input(i,1:5).^2*quad_p +
            5013.23;

        for j = 1:width(inter_p)
                for k = 1:height(inter_p)
                        pres_inter(j,k) = inter_p(j,k)*input(i,j)*input
                            (i,k);
                end
        end
        test_p(i) = sum(pres_inter, "all");
end
pressure = pressure+test_p;
Re_ratio = (D/D_paper).^n;
p_corrected = pressure.*transpose(Re_ratio);

%% Cut-off diameter
linear_d = [4.99523; 0.0987341; -2.24432; -0.0903146; 0.0111183];
quad_d = [
    -0.202652
     0.0822111
     0.988839
     0.0250071
    -0.000687999
];
inter_d = [
     0          0.469605   -2.06292    0.222628   0.00336809
```

```
    0          0          -0.203294   0.0372547  0.00498262
    0          0           0          -0.0208985  0.0070748
    0          0           0           0          -0.0225044
    0          0           0           0           0
];


for i = 1:height(input)
        diameter(i) = input(i,:)*linear_d + input(i,:).^2*quad_d +
            1.32318;

        for j = 1:width(inter_d)
                for k = 1:height(inter_d)
                        dia_inter(j,k) = inter_d(j,k)*input(i,j)*input(
                            i,k);
                end
        end
        test_d(i) = sum(dia_inter, "all");
end
diameter = diameter+test_d;

D_ratio = sqrt(D/D_paper);
D_corrected = diameter.*(D_ratio');

%% Calculate K
mu = 14.8E-6;                               % Viscosity gass
rho_p = 5242;                               % Density particle
rho_G = 1.225;                              % Density gass
g = 9.81;                                           % Gravitation

for i = 1:4
        syms K_hose
        functie =  @(Q, D_c, n, K) K * ((4*rho_G*Q) / (pi*mu*D_c)).^n
            * 0.5*rho_G .* (4*Q / (pi*D_c^2)).^2;
        K(i) = round(solve(functie(Q(i), D_c_K(i), n(i), K_hose) ==
            p_corrected(i)),2);
end

%%
disp("For Conf " + [1:height(input)]'+ ", the flow rate is "+ num2str(
    round(Q*1000*60)) + " l/min, pressure drop is " +  ...
        num2str(round(p_corrected', 0)) +" Pa, and cut-off diameter is
            " + ...
        num2str(round(D_corrected',3))+ " micrometer")

figure()
hold on
for i = 1:4
        Q_plot = [50:380]/60000;
        plot(Q_plot*60000, functie(Q_plot, D_c_K(i), n(i), K(i)))
end
legend('Conf 1', 'Conf 2', 'Conf 3', 'Conf 4', 'Location','northwest')
xlabel('Flow rate [l/min]')
ylabel('Pressure drop [Pa]')
title('Regression Model Pressure Drop')
% Karel
```

B.4 Matlab Code Cyclone Scale

```
1     clear all; clc; close all; warning('off')
2
3  % Input parameters:
4
5  mu = 14.8E-6;                    % Viscosity gass
6  rho_p = 5242;                    % Density particle
7  rho_G = 1.225;                   % Density gass
8  g = 9.81;                               % Gravitation
9
10 cyc_type = 5;
                                              % Type of cyclone used; see
      below
11 %                          D_i    D_o  l   L angle
12 cyc_para = [0.28, 0.34 0.4, 5, 20, 316, 0.134;
              % Riemeta
13                            0.133, 0.2, 0.33, 6.85, 9, 446.5, 0.323;
                                              % Bradley
14                            0.154, 0.214, 0.57, 7.43, 6, 6381, 0;
                                              % Mozley-1
15                            0.29, 0.2, 0.31, 4, 15, 2.618, 0.8;
                                              % Warman
16                            1/6, 0.2, 0.5, 4, 7.125, 6381, 0.0;
                                                  % Made cyclone
17                            0.36, 0.5, 0.5, 4, 7.125, 316, 0.134];
                                              % Excel Stairmand
18
19
20 c1 = cyc_para(cyc_type, 1);
21 c2 = cyc_para(cyc_type, 2);
22 c3 = cyc_para(cyc_type, 3);
23 c4 = cyc_para(cyc_type, 4);
24 angle = cyc_para(cyc_type, 5);
25 K = cyc_para(cyc_type, 6);
26 n = cyc_para(cyc_type, 7);
27
28 for i = 1:2
29 for j = 1:40
30         Q(i) = 100/60/1000*i;
31         D_c(j) = 0.03+0.001*j;
32
33 % Calculation pressure loss
34 v = 4*Q(i)/(pi*(D_c(j))^2);
35 Re = (rho_G*v*D_c(j))/mu;
36 dp_cyc(i,j) = K.*Re.^n .* 0.5 .* rho_G .* v.^2;
37
38 % Calculation efficiency
39 L = c4*D_c(j);
40 D_i = c1*D_c(j);
41 D_o = c2*D_c(j);
42 l = c3*D_c(j);
43
44 d_p50(i,j) = sqrt((36*(D_o/(2*D_c(j)))^2*(D_i/D_c(j))^4) / (pi*(L-l)/
      D_c(j)) * (mu*(D_c(j))^3)/((rho_p - rho_G)*Q(i)));
45 end
```

```
end

figure()
plot(Q*60000, d_p50*1e6)
xlabel("Flow rate [l/s]")
ylabel('Diameter [\mum]')
title('Cut-off diameter for varying cyclone diameter')
legend('D_c = 30 mm', 'D_c = 60 mm')

figure()
plot(Q*60000, dp_cyc)
xlabel("Flow rate [l/s]")
ylabel('Pressure [Pa]')
title('Pressure drop for varying cyclone diameter')
legend('D_c = 30 mm', 'D_c = 60 mm')

%%
close all
% Create the first plot
figure()
yyaxis left
plot(D_c*1000, d_p50*1e6)
xlabel("Diameter cyclone [mm]")
ylabel('Cut-off diameter [\mum]')
title('Cut-off diameter and pressure drop for varying flow rate')

% Create the second plot
hold on
yyaxis right
plot(D_c*1000, dp_cyc)
ylabel('Pressure [Pa]')
legend('Q = 100 l/s', 'Q = 200 l/s')
% Adjust the plot to accommodate both legends
fig = gcf;
fig.Position(3) = fig.Position(3) + 100;
```

B.5 Matlab Code Fit Experiment Data

```
    clc, close all, clear all


data = readtable("ExpData2.xlsx");
load('Hose_variables.mat');

D_c_input = [0.06, 0.065, 0.06, 0.065];

Q_min(:,1) = data.Q;                              % Flow rate data

Q = Q_min.*3./60./1000;                           % Flow rate from
   percentage to m^3/s

% Pressure short hose
delta_p(:,1) = (data.p1_no3)*100;        % Pressure data
delta_p(:,2) = (data.p2_no1)*100;
delta_p(:,3) = (data.p3_no1)*100;
delta_p(:,4) = (data.p4_no1)*100;
```

```
18
19 Q = Q(Q>0);
20
21 filtered_columns = cell(1, width(delta_p));
            % Remove Nan data from delta_p
22 for col = 1:width(delta_p)
23     col_non_nan = ~isnan(delta_p(:, col));
24     filtered_columns{col} = delta_p(col_non_nan, col);
25         dp(:,col) = filtered_columns{col};
26 end
27 delta_p = dp;
28
29 %%
30
31 %            D   Dc/D, D_i D_o  l    L  angle
32 dim_mark = [60, 1,    20, 30, 30, 240, 7.125];
33
34 for i = 3:length(dim_mark)-1
35         dim_mark(i) = dim_mark(i)/dim_mark(1);
36 end
37
38 mu = 14.8E-6;                              % Viscosity gass
39 rho_p = 5242;                              % Density particle
40 rho_G = 1.225;                             % Density gass
41 g = 9.81;                                          % Gravitation
42
43
44 %% Subtract piping losses
45 D_c_pipe = 0.06;
46 functie =  @(Q) K_hose * ((4*rho_G*Q) / (pi*mu*D_c_pipe)).^n_hose  *
       0.5*rho_G .* (4*Q / (pi*D_c_pipe^2)).^2;
47 dp_corrected = delta_p - functie(Q);
48
49 %% Find K and n
50 clc, close all
51
52 for i = 1:width(delta_p)
53         D_c = D_c_input(i);
54         v = @(Q) 4 * Q / (pi * D_c^2);
55         Re = @(Q) rho_G * (4 * Q / (pi * D_c^2)) * D_c / mu;
56         pressureLossFunction = @(x, Q) x(1) * ((4*rho_G*Q) / (pi*mu*D_c
              )).^x(2) * 0.5*rho_G .* (4*Q / (pi*D_c^2)).^2;
57
58
59
60         x0 = [6000, 0.01];
61         optimizedParams(i,:) = lsqcurvefit(pressureLossFunction,x0,Q,
              dp_corrected(:,i));
62
63         % Extract the optimized values of K and n
64         K_optimized(i) = optimizedParams(i,1);
65         n_optimized(i) = optimizedParams(i,2);
66
67         % R^2 calc
68         for j = 1:length(Q)
69                 pres_fit(j,i) = pressureLossFunction(optimizedParams(i
```

```
                    ,:),Q(j));
70          end
71
72          SStot(i) = sum((dp_corrected(:,i)-mean(dp_corrected(:,i))).^2);
                                % Total Sum-Of-Squares
73          SSres(i) = sum((dp_corrected(:,i)-pres_fit(:,i)).^2);
                                                % Residual Sum-Of-Squares
74          R2(i) = 1-SSres(i)/SStot(i);
                                                    % R^2
75  clc
76
77  % Plot data
78  figure(i)
79  plot(Q*1000*60,dp_corrected(:,i),'.',Q*1000*60,pressureLossFunction(
        optimizedParams(i,:),Q))
80  legend('Data','Fitted curve', 'Location','northwest')
81  title(['Data and Fitted Curve for Conf ', num2str(i)])
82  subtitle(['R^2 =' , num2str(R2(i)), ', K =' , num2str(round(K_optimized
        (i))), ', n = ', num2str(n_optimized(i))])
83  xlabel('Flow rate [l/s]')
84  ylabel('Pressure drop [Pa]')
85  end
86
87  %%
88  close all
89  figure(5)
90  hold on
91  legendentry = [];
92  for i = 1:width(delta_p)
93          plot(Q*1000*60, pressureLossFunction(optimizedParams(i,:),Q));
94          legendentry = [legendentry; 'Conf ', num2str(i)];
95  end
96  legend([legendentry], 'Location','northwest')
97  xlabel('Flow rate [l/min]')
98  ylabel('Pressure drop [Pa]')
99  title('Comparison Cyclone Configurations')
100
101 figure(6)
102 hold on
103 plot(Q*60000, delta_p)
104 plot(Q*60000, functie(Q))
105
106 legendentry = [legendentry; 'Pipe ', 0]
107 legend(legendentry, 'Location','northwest')
108 xlabel('Flow rate [l/min]')
109 ylabel('Pressure drop [Pa]')
110 title('Absolute pressure drop')
```

B.6 Comparison Experiment Data and Regression Model

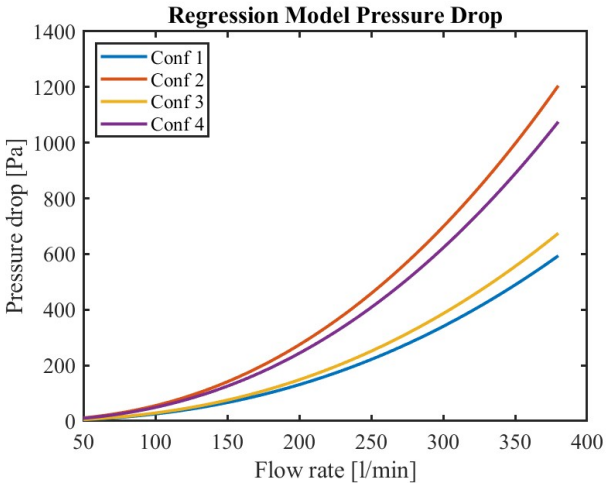

Figure B.2: Theoretical pressure drop (same as Figure 3.2)

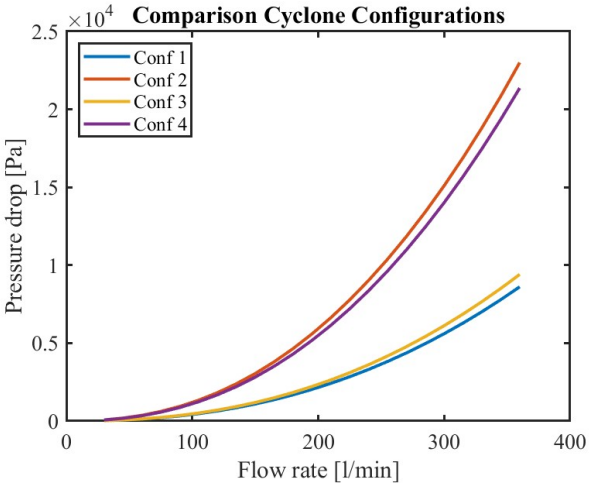

Figure B.3: Experimental pressure drop (same as Figure 4.11e)

C Appendix C

C.1 Building Setup

The building steps below are based on the schematic in Figure 4.8 and the material list in Table C.1. Steps 1 to 3 were already made in the lab by a previous lab user. During the installation, make sure all valves are closed unless mentioned otherwise. Teflon tape can be used on the threaded connection to make sure there is an air-tight seal. Do not use it however on the Swagelok fittings.

1. Connect the first pressure regulator to the valve at the air supply. Use Teflon tape to make an air-tight seal on the threads.
2. Connect a valve to the inlet side of the air tank and add a flexible 10 mm hose from the pressure regulator to the valve.
3. Add a third valve after the air tank. This should be within reach so the airflow can easily be stopped if needed.
4. Add the second pressure regulator after the third valve.
5. Connect the MFC to the pressure regulator using Swagelok fittings.
6. Connect a 12 mm flexible hose using Swagelok fittings to the outlet of the MFC. Make sure the hose can reach the position of the cyclone.
7. Cut 2 pieces of 8 cm length 12 mm flexible hose. Connect these using Swagelok to the inlet and outlet of the cyclone.
8. Add tee connectors to the short hoses connected to the cyclone. Connect the hose at the outlet of the MFC to the tee connector at the inlet of the cyclone.
9. Connect 20 cm pieces of 6 mm flexible hose to the third connector of the tee connectors. Use 10 to 6 mm push-in fittings for this.
10. Connect the 6 mm hoses to the pressure differential sensor. Ensure the inlet side hose is connected to the + of the sensor, and the outlet side to the - of the sensor.
11. Connect a 10 cm piece of 12 mm hose to the outlet side of the tee connector after the cyclone. This will be the air outlet of the system.
12. Set the first pressure regulator to a pressure of 1 bar. Open the first two valves. Check for air leaks. When no leaks are detected increase the pressure using the pressure regulator until 5 bar is reached.
13. Close the first valve and release the pressure using the pressure regulators. When all air is released, close the second valve.
14. Connect the MFC to the control box using the included cable. Use the USB cable to connect the control box to a computer.

Some of the experiments require the dispersion system. To add this to the setup follow the steps below.

1. Disconnect the 12 mm hose from the MFC to the first tee connection at the tee connector side.
2. Connect the end of the 12 mm hose from the MFC to the inlet of the dispersion system. This pushes on without threads or other clamps.
3. Connect a short 6 mm hose to the outlet of the dispersion system.
4. Use a 6 to 12 mm push-in connector and a 12 mm hose to connect the outlet of the dispersion system to the tee connector of the cyclone inlet.

The steps below show the preparations for an experiment. This includes connecting the required cyclone configuration and preparing the sensors.

- Connect the cyclone to be tested to the system. To disconnect a cyclone loosen the Swagelok connections at the inlet and outlet of the cyclone.
- Connect the computer to the control box and MFC. Make sure the flwo rate is set to 0%.
- Set both pressure regulators to 5 bar, and open the three valves.
- Set the flow rate to 20% for about 10 minutes. This warms up the MFC, for better results. Afterward, put it back to 0%.
- Turn on the pressure sensor. The pressure should read 0. If not, hold the "Tare" button for 5 seconds, which sets the pressure difference to zero.

C.2 Material List

Material	**Specifications / description**
Cyclone	4 different configurations
Pressure sensors	Electronic pressure differential sensors; range of 0 to 2 bar
Mass flow sensor	Range up to 300 l/min (CH_4)
Piping connections	Push-in and Swagelok
Flexible hoses	6 + 10 + 12 mm OD
Piping	12 mm OD
Pressurized air supply	At least 5 bar
Pressure regulators	Max input pressure 8 bar
Dispersion system	Suitable for iron powder
Ball valve	Rated for at least 8 bar
Labview	Version 2022Q3

Table C.1: Material list of setup

C.3 Experiment

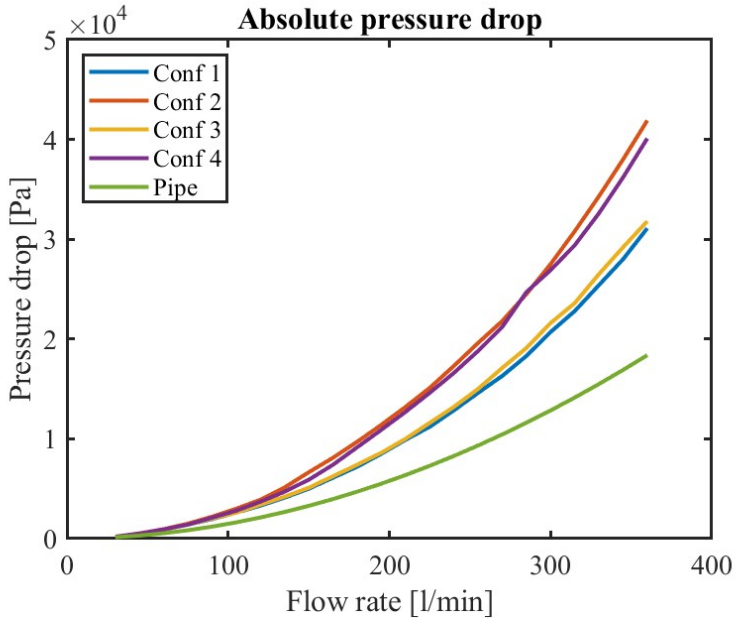

Figure C.1: Raw measured data from experiments 1-5